

Development of Surface-enhanced Raman Scattering Substrate Using Melt-blown Nonwoven Fabric Subjected to Electroless Ag Plating: A Basic Study

Yusuke Tahara,^{1,2*} Junya Yamamoto,¹ Takashi Nishiyama,²
Ren Tomisawa,¹ and Ryo Takigawa³

¹Graduate School of Science and Technology, Shinshu University,
3-15-1 Tokida, Ueda, Nagano 386-8567, Japan

²Department of Mechanical Engineering and Robotics, Faculty of Textile Science and Technology, Shinshu
University, 3-15-1 Tokida, Ueda, Nagano 386-8567, Japan

³Graduate School of Information Science and Electrical Engineering, Kyushu University,
744, Motoooka, Nishi-ku, Fukuoka 819-0395, Japan

(Received December 15, 2023; accepted February 9, 2024)

Keywords: surface-enhanced Raman scattering, melt-blown nonwoven fabric, polypropylene, electroless plating, hydrophobicity, Ag nanoparticles

The fabrication of the nanostructures required for surface-enhanced Raman scattering (SERS), which is increasingly used for chemical analysis, is complex and expensive. We demonstrated the feasibility of using low-cost, flexible SERS substrates produced using melt-blown nonwoven polypropylene (PP) fabrics as the base material. First, nonwoven PP fabrics with fiber diameters of $5.7 \pm 3.3 \mu\text{m}$ were prepared using the melt-blowing method. These fabrics were then hydrophilized using plasma treatment and densely modified with Ag nanoparticles with a diameter of approximately 90 nm by electroless plating involving a sensitization-activation process and the reduction of AgNO_3 . The SERS response of the Raman probe, 4-aminothiophenol (4-ATP), indicated that the resulting PP SERS substrates were more sensitive than a commercial low-cost SERS substrate made of laser nanopatterned soda lime glass coated with Ag in the concentration range of 10^{-4} – 10^{-6} M. The responses for 10^{-3} M 4-ATP after 3, 7, and 14 d were 103.0, 104.6, and 86.7%, respectively, based on the Raman peak at 1140 cm^{-1} measured on the day after fabrication (1 d). Thus, the fabricated PP SERS substrates are suitable for use as low-cost and flexible SERS substrates for chemical analysis.

1. Introduction

Raman spectroscopy is used extensively as a chemical analysis technique as it does not require complex pretreatments or labels, can be performed nondestructively, and allows highly sensitive measurements. Therefore, it is being used in combination with machine learning.^(1–3) Raman scattering, discovered by Raman⁽⁴⁾ in 1928, reflects the chemical structure, conformation, and intermolecular interactions of molecules as a Raman shift and has long been employed as a

*Corresponding author: e-mail: ytahara@shinshu-u.ac.jp
<https://doi.org/10.18494/SAM4820>

method for chemical analysis. Although the intensity of Raman scattering is very low, the presence of nanogaps and junctions in metallic nanoparticles and the shape and curvature of the nanometal surface⁽⁵⁾ induce an intense electric field owing to localized surface plasmon resonance, which significantly enhances the intensity of Raman scattering of the molecules present. This phenomenon is referred to as surface-enhanced Raman scattering (SERS). The small areas that considerably amplify this enhancement effect are referred to as hotspots. The SERS phenomenon⁽⁶⁾ is up to 10^{16} times more pronounced than Raman scattering and can be detected at the single-molecule level under ideal conditions.^(7–9) Thus, SERS has wide applicability in analytical chemistry, including cancer diagnosis,^(10,11) gas sensing,^(12,13) food safety and quality analysis,⁽¹⁴⁾ and drug analysis.⁽¹⁵⁾

Although SERS substrates are now available commercially, they require nanoscale surface treatments. Moreover, their fabrication involves semiconductor microfabrication techniques, such as lithographic methods and sputtering on glass and silicon wafers, to ensure consistent spectral enhancement.^(16,17) In addition, substrate manufacturing requires large amounts of organic solvents and involves complex processes, making it both time-consuming and expensive. To combine Raman spectroscopy with machine learning, which requires large amounts of high-quality data, for use in the field of chemical analysis, it is necessary to reduce the cost of SERS substrates, simplify their fabrication process, and improve their response reproducibility among different batches.

Substrates based on micro/nanofibers have been studied for use as flexible, low-cost, and high-sensitivity SERS substrates having a 3D structure.^(18–23) These include SERS substrates comprising electrospun nanofibers of poly(methyl methacrylate) modified with Ag nanoparticles (Ag NPs) by electroless plating,⁽²⁴⁾ SERS substrates comprising polypropylene (PP) films whose surfaces have been polymerized with poly(acrylic acid),⁽¹⁸⁾ SERS substrates comprising polyacrylonitrile-fiber-modified (3-aminopropyl) trimethoxysilane with Ag NPs,⁽¹⁹⁾ commercially available nonwoven fabrics polymerized with dopamine and plated with Ag in situ,⁽²⁰⁾ extremely low cost paper-based SERS substrates,⁽²¹⁾ poly(vinyl alcohol) electrospun nanofibers,⁽²²⁾ and bisphenol-A-sensing flexible SERS substrates comprising cellulose fibers made from waste paper.⁽²⁵⁾ These studies succeeded in increasing the hotspot density by exploiting the gaps between the fibers. Although there have been few studies on SERS substrates based on PP fiber, Bhandari *et al.*⁽²⁶⁾ fabricated a SERS substrate by physically depositing Ag onto a PP prefilter of 3M's High Performance Extraction Disc Cartridges.

We have been conducting research and development on the fabrication and structural analysis of nonwoven fabrics using the melt-blowing method.^(27,28) This method facilitates the control of the thickness, porosity, and weight by controlling parameters such as the die-to-collector distance (DCD), the air flow rate (AFR), and the power of the suction fan.^(29–31) The resulting nonwoven fabrics can have a fiber diameter distribution of 0.3–10 μm .⁽³⁰⁾ Melt-blown nonwoven fabrics have the following advantages for flexible SERS substrates: (1) Any thermoplastic polymer can be used, and polymer nonwoven fabrics with various chemical characteristics (charge and hydrophilicity/hydrophobicity) can be produced. (2) They are excellent as base materials for chemical measurements and do not require binders, additives, or secondary processes such as heat bonding. (3) Unlike electrospinning,^(32,33) the melt-blowing method is

environmentally friendly and does not require organic solvents. Moreover, it is superior to other micro/nanofiber-generating techniques, such as electrospinning, in terms of its large cost advantage and high production rate.⁽³¹⁾ (4) It can be employed in mass production. Furthermore, since it is used to manufacture medical masks and heating, ventilation, and air conditioning filters, it is easy to reduce manufacturing and supply costs. (5) The fibrous structure has a random pattern, and the surface-area-to-volume ratio is high.

The aim of this study was to demonstrate the feasibility of using low-cost, flexible SERS substrates using melt-blown nonwoven PP fabrics as the base material. We used PP as the base material for flexible SERS substrates owing to its desirable properties of tensile strength, impact strength, compressive strength, abrasion resistance, heat resistance, and biosafety.⁽³¹⁾ Although PP nonwovens are not suitable for single-molecule detection techniques because they are organic, they have the advantages described above. To the best of our knowledge, there are few reports on the use of melt-blown nonwoven PP fabrics as SERS substrates. To fabricate SERS substrates that enhanced the electric field, the hydrophobic nonwoven PP fabrics were modified with Ag via a plasma hydrophilization process, followed by Pd nucleation using a sensitization-activation method and electroless plating to achieve a structure consisting of a large number of Ag nanogaps. Surface observations were performed to evaluate the fabricated PP SERS substrates. Specifically, their Raman responses were measured using the Raman probe 4-aminothiophenol (4-ATP) and compared with those of a commercially available SERS substrate to evaluate their suitability for practical use as SERS substrates.

2. Materials and Methods

2.1 Reagents

Tin chloride, ethanol, and 4-ATP were obtained from Merck KGaA (Darmstadt, Germany). Palladium chloride, silver nitrate, ammonium hydroxide, glucose, and acetone were purchased from FUJIFILM Wako Pure Chemical Corporation (Osaka, Japan). The commercial SERS substrate RandaS⁽³⁴⁾ was purchased from AtoID Inc. The PP pellets were purchased from SunAllomer Ltd. (Tokyo, Japan). All aqueous solutions used in the experiments were prepared with pure water obtained using an Elix Essential system (Merck KGaA, Darmstadt, Germany).

2.2 Fabrication of melt-blown nonwoven PP fabrics

The melt-blown nonwoven PP fabrics were produced using a composite-type melt-blowing apparatus (MB-0300, Nippon Nozzle Co. Ltd., Kobe, Japan). An image of this instrument is shown in Fig. 1. The fabrication conditions were as follows. The nozzle angle was 60°, the setback distance was set at 0 mm, and the air gap distance was 0.5 mm. The width of the spinning nozzle was 400 mm, the nozzle having 438 holes with a hole diameter of 0.35 mm arranged at a pitch of 0.8 mm. The PP resin was spun at a rate of 0.15 g/min/hole.

The throughput PP resin was blown off at a spinning temperature of 280 °C with a hot-air flow rate of 250 m³/h. The rotation speed of the motor that controlled the air suction force was

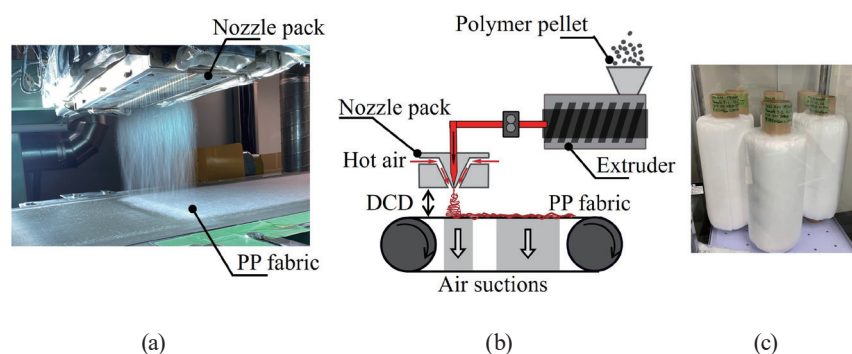


Fig. 1. (Color online) (a) Photograph of the melt-blowing apparatus, (b) schematic of the melt-blowing system, and (c) melt-blown PP nonwoven fabric.

set to 3500 rpm. The blown and drawn fibers were wound onto a conveyor at a speed of 1.7 m/min to form a web to produce the nonwoven fabric.

2.3 Ag modification by electroless plating

Previously,⁽³⁵⁾ we studied a method for modifying PP nonwoven fabrics with Ag NPs by dropping Ag NP solutions onto the nonwoven fabrics. However, because of the hydrophobicity of PP, the Ag NPs aggregate, and the response depends significantly on the modification location, making it impossible to obtain a stable SERS response. To solve this problem, we fabricated the SERS substrate with electroless plating on the fiber surface. Electroless Ag plating was performed on the hydrophobic nonwoven PP fabrics to form hotspots and fabricate the SERS substrates. The plating was performed using the conventional method via a sensitization-activation treatment,^(36–38) which involved a SnCl_2 – PdCl_2 process to form nanosize catalytic Pd nuclei on the surfaces of the fibers of the nonwoven PP fabrics. The reduction reaction of the Ag ions in the plating solution was followed by the formation of Ag NPs on the surface of the nonwoven PP fabrics. Plasma irradiation (YHS-R, SAKIGAKE-Semiconductor Co., Ltd., Osaka, Japan) was performed for 30 min to make the melt-blown nonwoven PP fabrics (5 mm × 5 mm) hydrophilic for the SnCl_2 – PdCl_2 process. Next, the hydrophilic nonwoven PP fabrics were immersed in a 3.0 M SnCl_2 solution for 30 min at room temperature. They were then immersed in a 3.0 M PdCl_2 solution for 30 min at room temperature. Electroless Ag plating was then performed, as previously described by Bao *et al.*⁽²⁴⁾ First, a 15 M ammonium hydroxide solution was added to 30 mL of 0.1 M AgNO_3 solution until the solution became clear. Next, 15 mL of 0.8 M potassium hydroxide solution was added to this mixture, followed by the dropwise addition of 15 M ammonium hydroxide solution until the mixture became clear. Then, 3 mL of 0.25 M glucose solution was added as a reducing agent, and the nonwoven fabrics were immediately immersed in the solution. Finally, following vigorous stirring with a magnetic stirrer for 20 s, the nonwoven PP fabrics were immersed in the solution for 25 s to form Ag NPs and the fabrics were subsequently used as SERS substrates. Prior to their use, the nonwoven PP SERS substrates were soaked in deionized water for 3 min, washed, and dried for 1 d.

2.4 Evaluation of hydrophobicity and surface observations

The water contact angle of the nonwoven PP fabrics was measured using a contact angle meter (CA-VP, Kyowa Interface Science Co., Ltd., Saitama, Japan) to confirm that the plasma treatment performed as a pretreatment before the electroless plating process had rendered them hydrophilic. The surface of the fiber structure of the nonwoven fabrics and the fabricated SERS substrate surfaces were observed using field-emission scanning electron microscopy (FE-SEM) and energy-dispersive X-ray spectroscopy (EDS) (JSM-IT800SHL JEOL, Ltd., Tokyo, Japan). The diameter of the fibers constituting the nonwoven fabrics was measured by FE-SEM. A sample piece was cut to 10×10 mm, and the machine direction–cross direction surface on the conveyor side was observed. The acceleration voltage was 10 kV and the working distance was approximately 10 mm. Sixteen imaging points were selected from the specimen, and SEM images were obtained at magnifications of 500 and 700 for each point. The diameters of all fibers (20–50 points) present in the $700\times$ magnification SEM image were measured until a total of 200 points were measured. Consequently, the average fiber diameter and fiber diameter distribution were determined. The size of the Ag NPs was evaluated from the FE-SEM images using ImageJ software. The basis weight (b_w) and thickness (t) of the obtained nonwoven fabrics were measured according to the International Organization for Standardization (ISO) 9073-1 and ISO 9073-2 standards, respectively.

2.5 SERS measurements

The Raman spectra were obtained with a Kaiser Hololab 5000 system (Kaiser Optical Systems, Inc., MI) using an excitation laser with a wavelength of 532 nm and a $10\times$ objective. The resolution was 4 cm^{-1} , the accumulation number was 1, the exposure time was 1 s, and the laser power was approximately 5 mW. The thickness of the fabricated PP SERS substrates was maintained at a constant value by sandwiching them along with 0.6 mm spacers between glass and stainless steel plates.

2.6 Measurement of 4-ATP

To evaluate the sensitivities of the fabricated PP SERS substrates, we evaluated their SERS responses using 4-ATP. The thiol group of 4-ATP binds strongly to Ag, forming a self-assembled monolayer (SAM). In addition, the benzene ring of 4-ATP exhibits high Raman intensity, rendering it suitable for use as a probe for evaluating SERS substrates.⁽³⁹⁾ The following experimental procedure was performed. The fabricated PP SERS substrate was immersed in 200 μL of a 4-ATP solution in ethanol for 30 min. The substrate was then removed and immersed in 200 μL of ethanol for 10 min to remove the unadsorbed 4-ATP. Next, the substrate was dried at room temperature for 1 h, and its Raman spectrum was measured. RandaS, a commercially available SERS substrate, was used for comparison. According to the data sheet, the substrate is made of laser nanopatterned soda lime glass, coated with Ag. The substrate is a low-cost SERS substrate and sold for 14 € on the market. Prior to their use, the substrates were immersed in

acetone, ethanol, and pure water for 10 min each, washed, and dried under N_2 . The measurements involving 4-ATP were performed as described above.

2.7 Stability of SERS substrates

The fabricated electroless-plated PP SERS substrates may exhibit low physical durability. There may also be a decrease in response due to the oxidation of Ag. Thus, to evaluate the stability of the SERS substrates, the Raman response of 10^{-3} M 4-ATP was measured using substrates stored at room temperature under dark conditions for 1, 3, 7, and 14 d after the substrate was fabricated. Here, the date of manufacture is set to 0 d. Measurements were conducted at four locations per SERS substrate using two substrates ($n = 8$).

3. Results and Discussion

3.1 Characteristics of melt-blown nonwoven PP fabric

The thickness, basis weight, and average fiber diameter of the prepared melt-blown nonwoven PP fabric were 0.89 ± 0.02 mm, 129 ± 3 g/m², and 5.7 ± 3.3 μ m, respectively. The fiber diameter distribution was 2–10 μ m, and several thermally fused fiber structures were observed (Fig. 2). The production cost of 1×1 mm² of the fabric for SERS measurements, including the PP pellets and electricity, was less than 0.10 USD in this study. The change in the contact angle of the fabric surface after the plasma treatment confirmed its hydrophilicity (Fig. 3). Before plasma irradiation, the contact angle was 136.2°, indicating strong hydrophobicity. In contrast, the contact angles after plasma treatment for 6, 10, and 12 min were 115.5, 108.5, and 44.6°, respectively. After 15 min of treatment, the contact angle was sufficiently low for the fabric to be completely penetrated by water droplets, indicating that it could be immersed in the plating solution for electroless plating.

3.2 Evaluation of melt-blown nonwoven PP fabrics after electroless Ag plating

Figure 4 shows FE-SEM images of PP nonwoven fabric prepared by the reduction of $AgNO_3$ without the $SnCl_2$ – $PdCl_2$ process, using the method discussed in Sect. 2.3. A thick Ag film was observed on the entire nonwoven fabric. It was confirmed that Ag powder would fall off the substrates that were not treated with the $SnCl_2$ – $PdCl_2$ process during washing after electroless plating or during the process of setting the substrates on the measurement jig. Therefore, we decided that the fabric was not suitable as an SERS substrate from the viewpoint of physical durability and SERS response variation. As the physical durability and response variation of this substrate were inadequate, electroless plating was performed via the $SnCl_2$ – $PdCl_2$ process in this study.

The SEM images confirmed that many Ag NPs, approximately 90 nm in size, were formed on the surfaces of the fibers of the melt-blown nonwoven PP fabric after electroless plating [Fig. 5(a)]. Agglomerates of the Ag NPs with a size of 1.5 μ m were also observed. As shown in Fig.

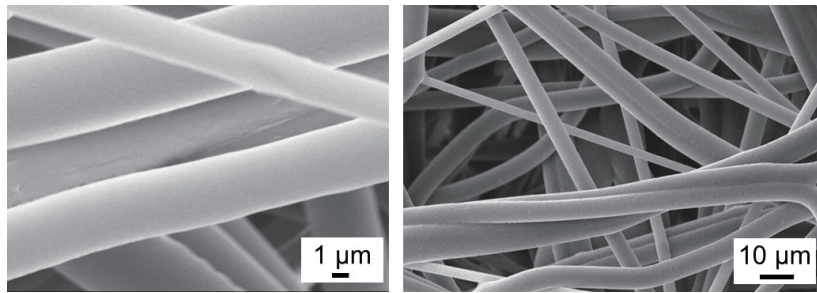


Fig. 2. FE-SEM images of the melt-blown nonwoven PP fabric.

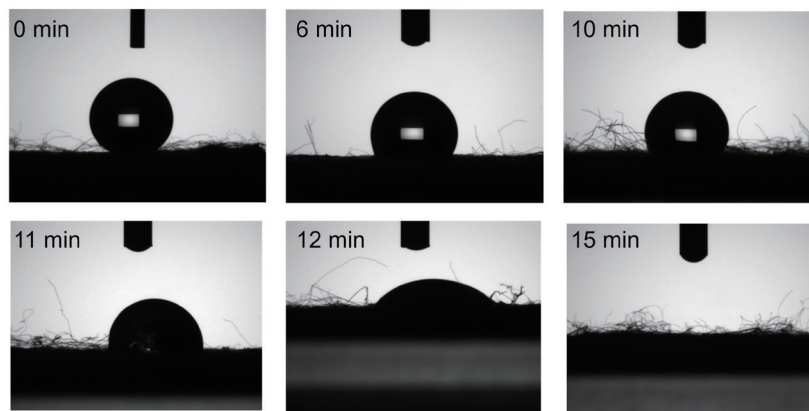


Fig. 3. Change in water contact angle of melt-blown nonwoven PP fabric after plasma treatment.

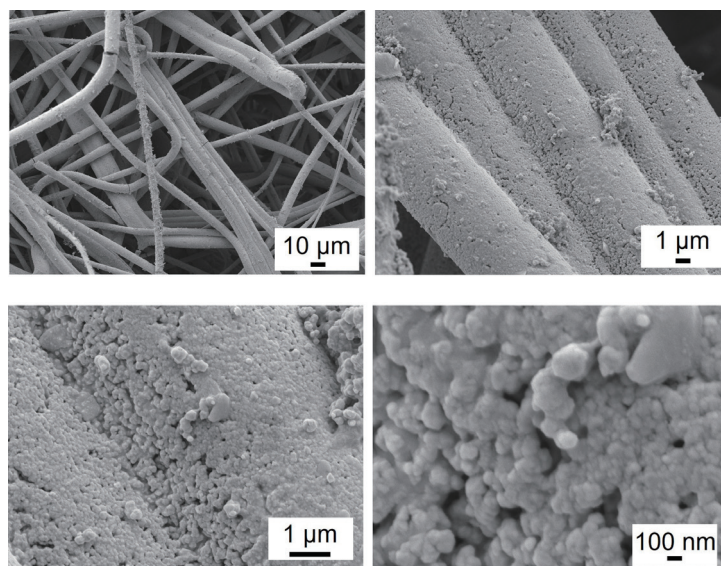


Fig. 4. FE-SEM images of Ag-modified melt-blown nonwoven PP fabric after electroless plating without SnCl₂-PdCl₂ process.

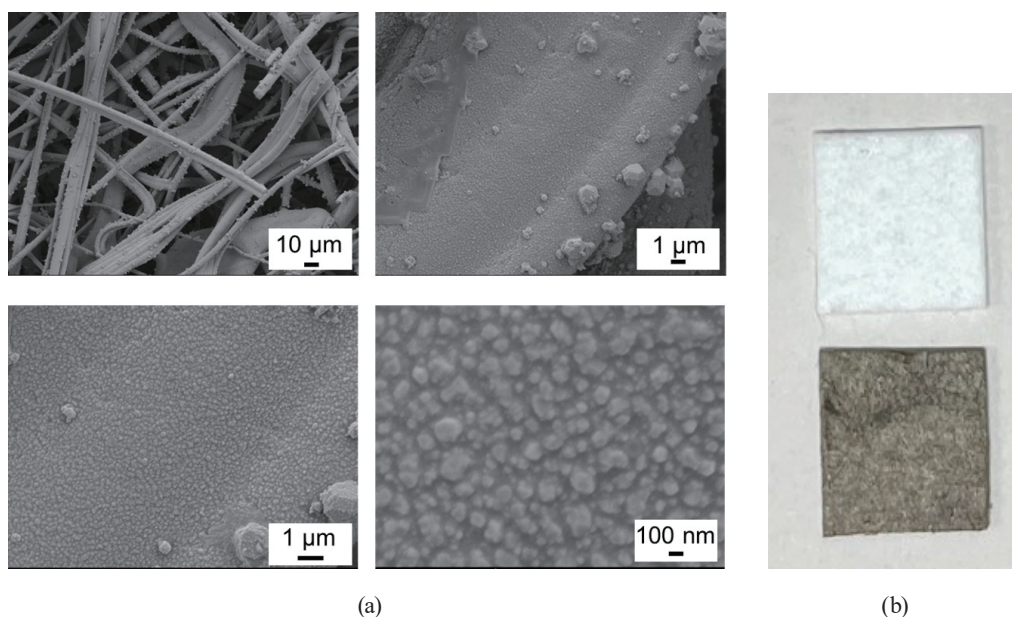


Fig. 5. (Color online) (a) FE-SEM images of Ag-modified melt-blown nonwoven PP fabric after electroless plating; (b) photographs of PP fabric before (top) and after (bottom) electroless plating (5 mm × 5 mm).

5(b), after electroless plating, the nonwoven PP fabric changed from white to gray owing to the Ag NPs. The EDS results confirmed the presence of Ag NPs and Pd (used as the catalyst) on the surfaces of the fibers. Thus, the post-plasma-treatment electroless plating performed using the sensitization-activation process resulted in the successful formation of Ag NPs on the hydrophilic surfaces of the fibers of the nonwoven PP fabric. However, the FE-SEM images do not indicate whether the Ag particles were formed by nucleation on the PP nonwoven fabric surface by the SnCl_2 - PdCl_2 process and/or they adhered to the PP nonwoven fabric after the Ag particles were nucleated. Thus, a more detailed chemical structure analysis is required for further clarification. The EDS analysis also indicated the presence of C along with the Ag NPs after the electroless plating. This C was assumed to be from the PP. In addition, Cl from the tin chloride solution, Pd from the palladium chloride solution, and K from the potassium hydroxide were observed.

3.3 SERS response of 4-ATP

The fabricated PP SERS substrate was immersed in a 4-ATP solution, resulting in the adsorption of 4-ATP on the Ag NPs. This was followed by the removal of the unadsorbed 4-ATP molecules by immersion in ethanol. Therefore, the Raman intensity reflected the amount of 4-ATP adsorbed on the Ag NPs, which indicated the extent of Ag modification of the nonwoven PP fabric and the number of Raman hotspots formed. Figure 6 shows the Raman spectrum of 10^{-3} M 4-ATP on the fabricated SERS substrate; for comparison, the Raman spectra of a bulk solution of 10^{-3} M 4-ATP in ethanol and PP pellets are also shown. The increase in the baseline of the Raman spectrum of 4-ATP could be mainly due to the light scattering caused by the

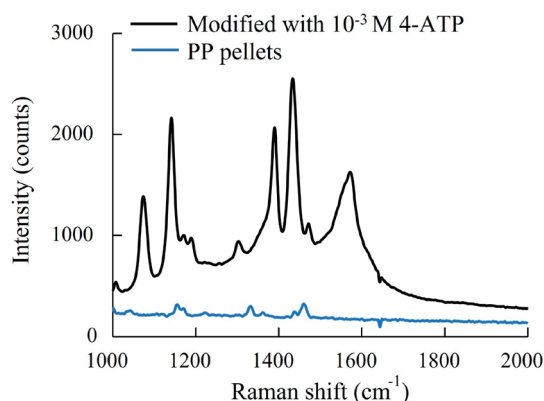


Fig. 6. (Color online) Raman spectra of fabricated PP SERS substrate modified with 10^{-3} M 4-ATP, bulk solution containing 10^{-3} M 4-ATP, and PP pellets.

surface roughness and 3D structure of the nonwoven fabric. Peaks were observed at 1075 (C–S stretching vibrations), 1140 (C–C stretching), 1390 (C–H band), 1438 (benzene ring breathing motion), and 1583 cm^{-1} (C=C band).⁽⁴⁰⁾ These results confirmed that the chemically modified melt-blown nonwoven PP fabric exhibited SERS activity. Considering that the nonwoven PP fabric was fabricated without the use of any special additives⁽³¹⁾ and was free of impurities that could adversely affect its Raman spectrum, it is highly suited for use as a SERS substrate. Figure 7(a) shows the raw data without baseline correction of the Raman spectra of the fabricated PP SERS substrate after being modified with 4-ATP solutions with concentrations of 10^{-3} – 10^{-7} M. Figure 7(b) shows the spectra and data for the commercial SERS substrate. The Raman spectra of both SERS substrates contained peaks at similar positions, and the Raman peak intensity increased with increasing 4-ATP concentration, confirming that the intensity depended on the concentration. For the fabricated PP SERS substrate, we expected to observe a Raman peak related to PP⁽⁴¹⁾ as the concentration of 4-ATP decreased. However, no such peak was observed, even in the case of 10^{-7} M 4-ATP. This spectrum shows the baseline signal of the fabricated PP SERS substrate. Therefore, the laser intensity, irradiation time, and integration were not affected by the PP polymer.

The intensities of the peak at 1140 cm^{-1} in the Raman spectra, corresponding to the different 4-ATP concentrations, are shown in Fig. 8. The peak intensity was calculated by Igor Pro (WaveMetrics, Inc.). At the concentration of 10^{-3} M, the Raman spectral intensity for the commercial SERS substrate was higher than that for the fabricated PP SERS substrate, whereas at the lower concentrations (10^{-4} to 10^{-6} M), the fabricated PP SERS substrate exhibited higher Raman spectral intensities than those for the commercial SERS substrate and hence higher sensitivity. This was probably because the number of effective Raman hotspots and the effective surface curvature of the Ag surface within the detection range of the fabricated PP SERS substrate were greater than those of the commercial SERS substrate. In the enlarged image of Fig. 5 (a, bottom right), gaps of approximately 10–100 nm are observed between the particles [Fig. 9(a)]. Some particle clusters with sizes on the order of tens of nanometers are also observed [Fig. 9(b)]. Therefore, the electroless-plated SERS substrate is likely to have hotspots and rough

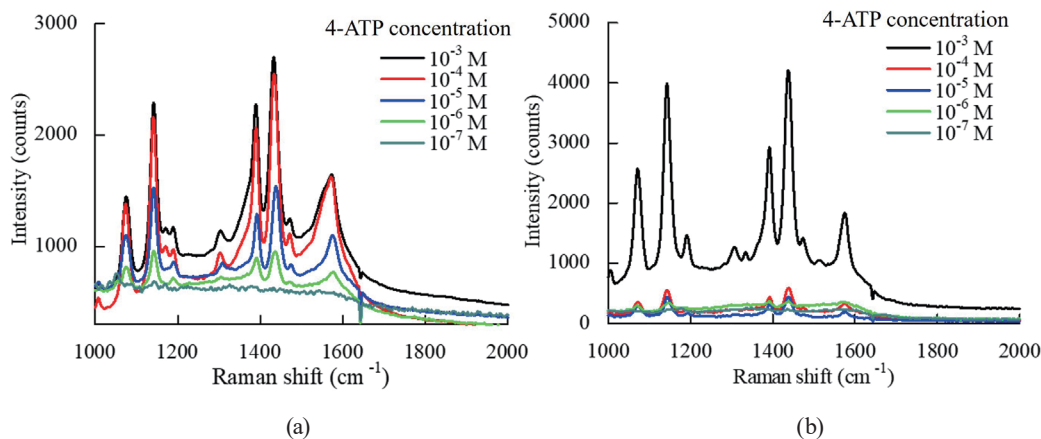


Fig. 7. (Color online) Raman spectra of (a) fabricated PP SERS substrate; (b) commercial SERS substrate after modification with 4-ATP.

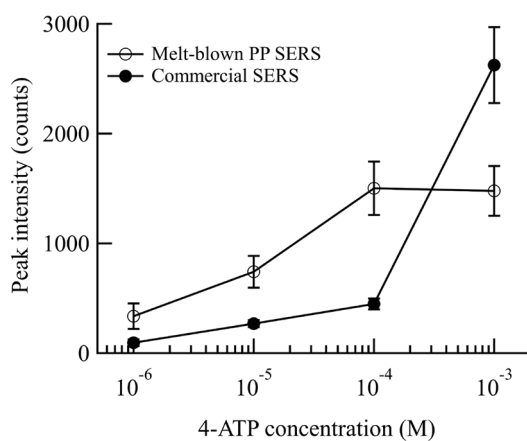


Fig. 8. Intensities of peak at 1140 cm^{-1} of fabricated PP SERS and commercial SERS substrates after modification with 4-ATP. Data are presented as mean \pm standard deviation (SD).

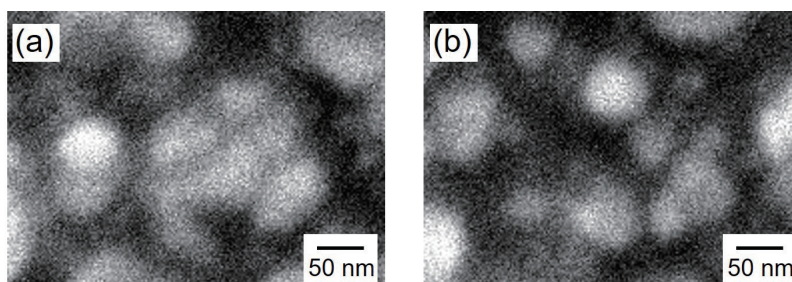


Fig. 9. Enlargement of the SEM image in Fig. 5(a, bottom right). (a) Approximately 10–100 nm gaps between the particles and (b) particle clusters with sizes on the order of tens of nanometers.

metal surfaces that are effective for SERS responses. To increase the sensitivity for optimizing the electroless plating method, it is necessary to examine the surface of Ag particles and the gap distance between particles on the fiber by scanning probe microscopy. In addition, the molecular adsorption capacity of the nonwoven fabric may also have been higher. Therefore, the 3D structure of the melt-blown nonwoven PP fabric and its Ag modification via electroless plating resulted in a highly sensitive SERS substrate for measuring 4-ATP, although further analysis of the relationship with the 3D structure is needed. However, a comparison of the coefficient of variation (CV) values of the fabricated nonwoven and commercial SERS substrates showed that the CV of the former was approximately 5% higher for all concentrations except 10^{-6} M. The CVs were calculated using data values measured at random locations on the substrate ($n = 6$). This result indicates that the porosity of the nonwoven fabric caused variations in its Raman peak intensity based on the position of laser irradiation. Owing to the presence of gaps between the fibers, the peak intensity is lower when the laser is irradiated on fibers that are not at the proper focal distance, in contrast to the case for measurements performed at the proper focal distance. In addition, the difference in response due to capillary action caused by the nonwoven structure should be investigated. Although the sensitivity of the measurement is reduced by extending the detection range of laser irradiation and scattered light, the variation may also be reduced. Moreover, the relationship between the peak intensity and the depth direction can be investigated and reflected in the design guidelines for nonwoven fabrics. In the case of melt-blown fabrics, the fiber diameter can be reduced by increasing the DCD and AFR. An increase in the AFR increases the weight of fibers and the distance between them. In the future, we will attempt to optimize the fiber diameter and interfiber distance during the fabrication of the melt-blown nonwoven fabric to reduce the variation arising from changes in the measurement position. In the present study, we performed an evaluation using 4-ATP, a Raman probe that strongly binds to Ag. To further demonstrate the utility of this SERS substrates, it is necessary to evaluate the SERS response to analytes with other chemical characteristics along with the relationship between the PP nonwoven structure and the chemical characteristics of the analytes.

3.4 Stability of SERS substrates

The responses after 3, 7, and 14 d were 103.0, 104.6, and 86.7%, respectively, relative to the Raman peak at 1140 cm^{-1} measured on the day after fabrication (1 d) (Fig. 10). It is generally believed that the sensitivity of SERS substrates is decreased by contamination in the air or via oxidation. In addition, we considered that electroless-plated SERS substrates might be physically brittle, although they still exhibited a high response after one week. Commercially available SERS substrates are sold in hermetically sealed packaging to prevent oxidation; however, this experiment was conducted at room temperature in the dark. Although the response of the prototype SERS decreased to 86.7% after two weeks, the sensitivity of the response was considered to be sufficiently high for use in measurements. Shao *et al.*⁽³²⁾ reported that a SERS substrate comprising Ag and a poly(styrene-*co*-butadiene) fibrous membrane stored in N_2 at $4\text{ }^\circ\text{C}$ exhibited 87.2% of the original Raman intensity after 28 d, which indicated greater stability than that when maintained under an ambient atmosphere. Therefore, the use period of the fabricated SERS substrates can be further extended by optimizing the storage method.

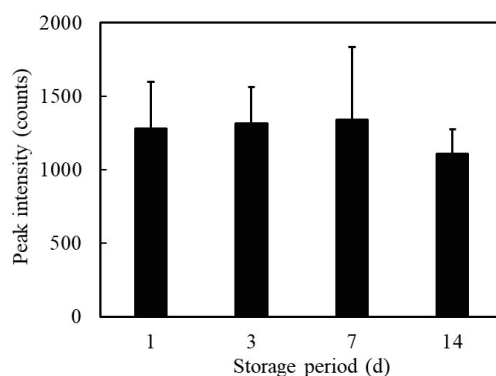


Fig. 10. Intensities of the peak at 1140 cm^{-1} of the fabricated PP SERS for 10^{-3} M 4-ATP. The storage times were 1, 3, 7, and 14 d after the modification day. Data are presented as mean \pm standard deviation (SD). Measurements were conducted at four locations per SERS substrate using two substrates ($n = 8$)

4. Conclusions

We demonstrated the feasibility of a novel SERS substrate based on a melt-blown nonwoven PP fabric by electroless plating Ag NPs on the fabric. There have been no reports of SERS substrates using nonwoven fabrics made by the melt-blowing method. The fabricated PP SERS substrate exhibited good sensitivity to the Raman probe 4-ATP, which acted as a SAM for Ag. The Raman responses of the fabricated SERS substrate were 104.6 and 86.7% after one and two weeks of storage at room temperature, respectively. Although single-molecule detection is difficult because of the use of organic molecules, the fabricated substrates are very suitable for use as low-cost SERS substrates with good sensitivity and stability. The melt-blowing method can be used for the mass production of SERS substrates from thermally molten resins without requiring the use of organic solvents and thus should also be suitable for producing SERS substrates from materials other than PP. In the next step, we will attempt to optimize the fiber diameter and fiber-to-fiber distance of the melt-blown nonwoven fabric to increase the sensitivity and repeatability of the resulting SERS substrate.

Acknowledgments

The authors thank Prof. T. Matsui, Prof. K. Toko, Prof. T. Rikitake, Dr. M. Tanaka, Dr. T. Onodera and Dr. K. Sanematsu of the Research and Development Center for Five-Sense Devices, Kyushu University, Japan, and MD. H. Sonoda and MD. K. Nonaka of the Department of Surgery and Science, Graduate School of Medical Sciences, Kyushu University, Japan for helpful discussion and advice. This study was supported by JSPS KAKENHI (grant numbers 21H03798 and 23K03881) and used research equipment shared in the MEXT Project for Promoting Public Utilization of Advanced Research Infrastructure (a program for supporting the construction of core facilities) Grant Number JPMXS0441000021.

References

- 1 W. J. Thrift and R. Ragan: *Anal. Chem.* **91** (2019) 13337. <https://doi.org/10.1021/acs.analchem.9b03599>
- 2 F. Lussier, D. Missirlis, J. P. Spatz, and J.-F. Masson: *ACS Nano.* **13** (2019) 1403. <https://doi.org/10.1021/acsnano.8b07024>
- 3 J. Son, G.-H. Kim, Y. Lee, C. Lee, S. Cha, and J.-M. Nam: *J. Am. Chem. Soc.* **144** (2022) 22337. <https://doi.org/10.1021/jacs.2c05950>
- 4 C. V. Raman: *Proc. Indian Acad. Sci., Sect. A* **37** (1953) 333. <https://doi.org/10.1007/BF03052651>
- 5 N. Guillot and M. L. de la Chapelle: *J. Quant. Spectrosc. Radiat. Transfer* **113** (2012) 2321. <https://doi.org/10.1016/j.jqsrt.2012.04.025>
- 6 S. E. J. Bell, G. Charron, E. Cortés, J. Kneipp, M. L. de la Chapelle, J. Langer, M. Procházka, V. Tran, and S. Schlücker: *Angew. Chem. Int. Ed.* **59** (2020) 5454. <https://doi.org/10.1002/anie.201908154>
- 7 K. Kneipp, Y. Wang, H. Kneipp, L. T. Perelman, I. Itzkan, R. R. Dasari, and M. S. Feld: *Physic. Rev. Lett.* **78** (1997) 1667. <https://doi.org/10.1103/PhysRevLett.78.1667>
- 8 E. C. L. Ru and P. G. Etchegoin: *Annu. Rev. Phys. Chem.* **63** (2012) 65. <https://doi.org/10.1146/annurev-physchem-032511-143757>
- 9 Y. Qiu, C. Kuang, X. Liu, and L. Tang: *Sensors* **22** (2022) 4889. <https://doi.org/10.3390/s22134889>
- 10 M. Blanco-Formoso and R. A. Alvarez-Puebla: *Int. J. Mol. Sci.* **21** (2020) 2253. <https://doi.org/10.3390/ijms21062253>
- 11 J. B. Phyto, A. Woo, H. J. Yu, K. Lim, B. H. Cho, H. S. Jung, and M.-Y. Lee: *Anal. Chem.* **93** (2021) 3778. <https://doi.org/10.1021/acs.analchem.0c04200>
- 12 J. Prakash, P. R. de Oliveira, H. C. Swart, M. Rummyantseva, M. Packirisamy, B. C. Janegitz, and X. Li: *Sens. Diagn.* **1** (2022) 1143. <https://doi.org/10.1039/D2SD00133K>
- 13 L. Chen, H. Guo, F. Sassa, B. Chen, and K. Hayashi: *Sensors* **21** (2021). <https://doi.org/10.3390/s21165546>
- 14 A. Nilghaz, S. Mahdi Mousavi, A. Amiri, J. Tian, R. Cao, and X. Wang: *J. Agric. Food Chem.* **70** (2022) 5463. <https://doi.org/10.1021/acs.jafc.2c00089>
- 15 A. G. Berger, S. M. Restaino, and I. M. White: *Anal. Chim. Acta.* **949** (2017) 59. <https://doi.org/10.1016/j.aca.2016.10.035>
- 16 M. S. Schmidt, J. Hübner, and A. Boisen: *Adv. Mater.* **24** (2012) OP11. <https://doi.org/10.1002/adma.201103496>
- 17 M. Fan and A. G. Brolo: *Phys. Chem Chem. Phys.* **11** (2009) 7381. <https://doi.org/10.1039/B904744A>
- 18 A. A. Gorbachev, I. A. Khodasevich, and O. N. Tretinnikov: *J. Appl. Spectrosc.* **87** (2020) 249. <https://doi.org/10.1007/s10812-020-00992-6>
- 19 L. Cai, Z. Deng, J. Dong, S. Song, Y. Wang, and X. Chen: *J. Anal. Test.* **1** (2017) 322. <https://doi.org/10.1007/s41664-017-0035-3>
- 20 Z. Zhang, T. Si, J. Liu, and G. Zhou: *Nanomaterials* **9** (2019) 384. <https://doi.org/10.3390/nano9030384>
- 21 N. Chamuah, A. Hazarika, D. Hatiboruah, and P. Nath: *J. Phys. D: Appl. Phys.* **50** (2017) 485601. <https://doi.org/10.1088/1361-6463/aa8fef>
- 22 Y. Chen, G. J. Huang, and Y. Li: *Dig. J. Nanomater. Biostruct.* **17** (2022) 1275. <https://doi.org/10.15251/djnb.2022.174.1275>
- 23 G. J. Huang, Y. M. Chen, and Y. Y. Li: *Dig. J. Nanomater. Biostruct.* **17** (2022) 171. <https://doi.org/10.15251/DJNB.2022.171.171>
- 24 Y. Bao, C. Lai, Z. Zhu, H. Fong, and C. Jiang: *RSC Adv.* **3** (2013) 8998. <https://doi.org/10.1039/C3RA41322E>
- 25 S. Liu, R. Cui, Y. Ma, Q. Yu, A. Kannegulla, B. Wu, H. Fan, A. X. Wang, and X. Kong: *Spectrochim. Acta, Part A.* **227** (2020) 117664. <https://doi.org/10.1016/j.saa.2019.117664>
- 26 D. Bhandari, M. J. Walworth, and M. J. Sepaniak: *Appl. Spectrosc.* **63** (2009) 571. <https://doi.org/10.1366/000370209788347002>
- 27 N. Koike, R. Tomisawa, T. Ikaga, K. Kim, Y. Ohkoshi, K. Okada, H. Masunaga, T. Kanaya, H. Katsuta, and Y. Funatsu: *J. Fiber Sci. Technol.* **76** (2020) 161. <https://doi.org/10.2115/fiberst.2020-0019>
- 28 R. Tomisawa, A. Makimura, K. H. Kim, and Y. Ohkoshi: *J. Tex. Eng.* **69** (2023) 71. <https://doi.org/10.4188/jte.69.71>
- 29 S. J. Russell, A. Wilson, A. Brydon, A. Pourmohammadi, C. White, G. Bhat, S. R. Malkan, S. Anand, D. Brunnschweiler, G. Swarbrick, S. Russell, A. Pourmohammadi, R. A. Chapman, A. Idris Ahmed, N. Mao, S. J. Russell, and B. Pourdeyhimi: Contributor contact details (Woodhead Publishing, 2007) pp. 172 and 409.
- 30 T. Ishikawa, Y. Ishii, Y. Ohkoshi, and K. H. Kim: *Text. Res. J.* **89** (2019) 1734. <https://doi.org/10.1177/0040517518779255>
- 31 Y. Kara and K. Molnár: *J. Ind. Text.* **51** (2022) 137S. <https://doi.org/10.1177/15280837211019488>

- 32 F. Shao, J. Cao, Y. Ying, Y. Liu, D. Wang, X. Guo, Y. Wu, Y. Wen, and H. Yang: *Sensors* **20** (2020). <https://doi.org/10.3390/s20154120>
- 33 W. H. Skinner, M. Chung, S. Mitchell, A. Akidil, K. Fabre, R. Goodwin, A. A. Stokes, N. Radacsi, and C. J. Campbell: *Anal. Chem.* **93** (2021) 13844. <https://doi.org/10.1021/acs.analchem.1c02530>
- 34 W. Schweikert, F. Schnürer, A. Mendl, and S. Müller: *SPIE Security + Defence* **11166** (2019). <https://doi.org/10.1117/12.2532780>
- 35 N. Takashi, Y. Junya, T. Ren, T. Ryo, and T. Yusuke: *Proc. 39th Sens. Symp. Sens., Micromach. Appl. Syst. (IEEJ, 2022)*, 14P5-P-46, 4p (in Japanese).
- 36 R. L. Meek: *J. Electrochem. Soc.* **122** (1975) 1478. <https://doi.org/10.1149/1.2134045>
- 37 M. Charbonnier, M. Alami, and M. Romand: *J. Appl. Electrochem.* **28** (1998) 449. <https://doi.org/10.1023/A:1003204909001>
- 38 L. Wei, J. Yu, X. Hu, R. Wang, and Y. Huang: *Chin. J. Chem. Eng.* **24** (2016) 1154. <https://doi.org/10.1016/j.cjche.2016.04.008>
- 39 Y. Wang, H. Chen, S. Dong, and E. Wang: *J. Chem. Phys.* **124** (2006) 074709. <https://doi.org/10.1063/1.2172591>
- 40 J. Zhu, N. Wu, F. Zhang, X. Li, J. Li, and J. Zhao: *Spectrochim. Acta, Part A* **204** (2018) 754. <https://doi.org/10.1016/j.saa.2018.06.105>
- 41 A. S. Nielsen, D. N. Batchelder, and R. Pyrz: *Polymer.* **43** (2002) 2671. [https://doi.org/10.1016/S0032-3861\(02\)00053-8](https://doi.org/10.1016/S0032-3861(02)00053-8)